DNA Condensation

Matej Marinč
Advisor: prof. Rudi Podgornik

19th March 2002

Abstract

Recent studies of DNA condensation are reviewed. First, different intrachain interactions (based on DNA - DNA interactions and DNA - counterions interactions) providing a general mechanism to condensation have been described. Experimentally obtained structures of condensed DNA are compared with the simple computer simulations of stiff polyelectrolyte. Later, the formation of toroid is explained on the basis of the mathematical approach. DNA molecule has been treated as an inextensible chain, where all the interactions are mediated by a single monomer-monomer interaction potential. Finally, the packaging of DNA molecules in the viral capsids as an in vivo realization of the DNA condensation is described.

Contents

1 Introduction

DNA condensation is the collapse of extended DNA chains into compact, orderly particles containing only one or a few molecules. The decrease in size of the DNA domain and the toroidal shape of condensed particles are both striking, so the phenomenon of DNA condensation has drawn considerable attention.

DNA molecule is a long negatively charged polyelectrolyte (polymer having charged monomers). It is relatively stiff due to its double helical structure shown on Figure 3. It has to fit into a very small space inside a cell or a virus capsid. The size of viral DNA is, for example, on the order of several μm, yet it has to fit in a virus capsid about 100 nm in diameter. The same happens with larger DNA molecules being built in chromosome. For example, bacterial DNA E.*coli* extends 1 mm, yet it must fit into a nucleolar region about 1. Countour length of a human DNA is a few cm. μm across.

viral DNA	several μm
bacterial DNA	several mm
human DNA	several cm

Figure 1: Tipical lengths of different DNA molecule.

countour length of viral DNA	several μm
diameter of viral capsid	100 nm
diameter of DNA	2 nm
persistence length L_P	50 nm
1 basepair	0.34nm
1 effective charge	0.17 nm

Figure 2: Tipical parameters of all DNA molecules.

2 Energetics of DNA condensation

Considering the obvious energetic barriers to such tight packaging - the loss of configurational entropy of the long DNA molecule, the tight bending of the stiff double helix, the electrostatic repulsion of the negatively charged DNA monomers - it is a great surprise that DNA condensation can occur spontaneously in the presence of low concentration of multivalent cations.

2.1 Electrostatic Interactions

Parts of DNA molecules in aqueous solution of cations interact with themselves and with the counterions via Coulomb potential

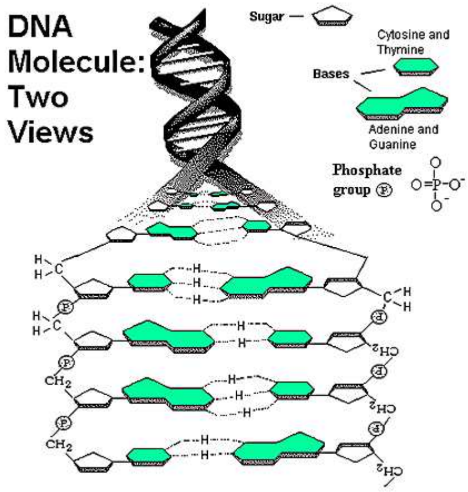

Figure 3: DNA structure. *http: //www.accessexcellence.org/AB/GG/dna_ molecule.html*

$$U_C = \frac{z^2 e_0^2}{4\pi\epsilon\epsilon_0}\frac{1}{r}. \tag{1}$$

In almost all cases DNA is surrounded with water. Electrostatic interactions are thus much weaker ($\epsilon = 80$ for water). Still, the coulomb interaction is very long-ranged, such that many particles are coupled due to their simultaneous electrostatic interactions. Electrostatic problems are therefore typically many-body problems, very difficult to solve. Anyway, two theories successively describe limiting behaviours. Poisson Boltzmann approach is valid for weakly charged objects and low-valent counterions, while the opposite limit of highly charged objects and high-valent counterions is accurately described by strong coupling theory.

2.1.1 Poisson-Boltzmann theory

Starting first with Poisson-Boltzmann (PB) theory let us consider spherical macroion surrounded with oppositely charged ions. A charge of the macroion equals to the sum of charges of all counterions. The macroion and the cunterions define effective electric potential which is given by Poisson equation:

$$\nabla^2 U = -\frac{\rho_e}{\epsilon\epsilon_0} = -\frac{z e_0 \rho_0 \exp[-\beta e_0 U(r)]}{\epsilon\epsilon_0}, \tag{2}$$

where z is the valence of the counterions. Counterions surround macroion according to Boltzmann distribution if their motion is free enough. This is Poisson Boltzmann (PB) approximation. Similarly, Debye-Hückel potential is obtained, however, in that case macroion is surrounded by a salt, which means, by positively and negatively charged ions, whereas in our case only the counterions are present in the solution.

Equation 2 for two charged plates embedded into solution of oppositely charged counterions has to be solved in one dimension. There are few parameters that characterizes the length scales of different interactions. First, Bjerrum length measures the distance at which two unit charges interact with thermal energy (in water $l_B = 0.7\mathrm{nm}$) $l_B = \frac{e_0^2}{4\pi\epsilon k_B T}$. Second, Gouy-Chapman length $\mu = 1/2\pi z \sigma l_B$ measures the distance from the wall at which the potential energy of an ion reaches the termal energy. The coupling constant $\Xi = \frac{l_B z^2}{\mu} = 2\pi z^3 l_B^2 \sigma$ connects both characteristic length constants. If the plates are weakly charged and if the counterions have low valence, the counterions interact weakly between themselves. They behave similar to gas molecules. Thus PB approximation is valid in the limit $\Xi \ll 1$.

Substitution $\beta e_0 U(r) = U_1(r)$ leads to the PB equation

$$\frac{\partial^2 U_1}{\partial x^2} = \kappa^2 e^{-U_1}, \tag{3}$$

where $\kappa^2 = \frac{\rho_0 e_0^2}{\epsilon\epsilon_0 k_B T}$. The symmetric solution of this differential equation (plates are at $x = 0$ and at $x = d$) is

$$U_1(x) = 2 \ln \cos \left[\frac{\kappa}{\sqrt{2}} (x - d/2) \right] \tag{4}$$

By considering Boltzmann distribution of counterions in the potential given by Equation 4, PB result for the density of counterions is achieved.

$$\rho = z e_0 \rho_0 e^{-U_1} = z e_0 \rho_0 / \cos^2 \left[\frac{\kappa}{\sqrt{2}} (x - d/2) \right], \tag{5}$$

The pressure between the plates can be calculated according to gas theorem:

$$\begin{aligned} p &= kT\rho(x = 0) = k_B T \rho_0 e^{-U_1} & (6) \\ &= \frac{k_B T \epsilon\epsilon_0}{e_0 k_B} \kappa^2 & (7) \end{aligned}$$

The total charge of counterions has to be oppositely the same as charge of both plates. The normalization condition $\int \sigma \mathrm{d}S = \int \rho \mathrm{d}V$ leads to the equation for κ:

$$\kappa \tan \frac{\kappa d}{2} = 1. \tag{8}$$

Assimptotic values for κ and P are

$$\begin{array}{lllll} d & \to & 0 & \frac{\kappa^2 d}{2} = 1 & \Rightarrow \quad \kappa^2 \sim 1/d, P \sim 1/d \\ d & \to & \infty & \frac{\kappa d}{2} = \pi/2 & \Rightarrow \quad \kappa \sim 1/d, P \sim 1/d^2 \end{array}$$

In PB approximation pressure between plates is always repulsive. Two limits given above may be observed on the (Figure 4, bold line). At small separations $d \to 0$ pressure is highly repulsive (as a function $P \sim 1/d$), whereas at large separations the repulsive pressure goes to zero.

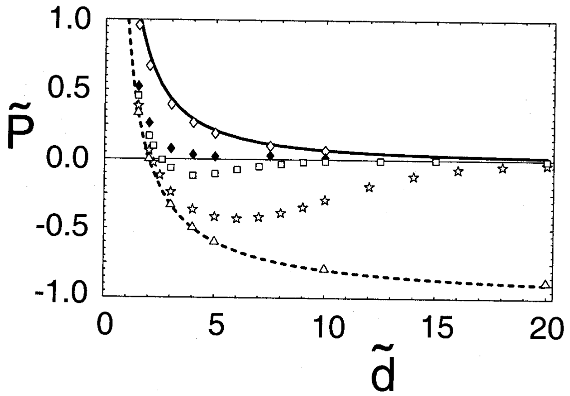

Figure 4: Monte Carlo simulations result for rescaled pressure $P_1 = P/2\pi l_B\sigma^2$ as a function of the rescaled plate separation $d_1 = d/\mu$. Symbols correspond to coupling parameters $\Xi = 0.5$ (open diamonds), $\Xi = 10$ (filled diamonds), $\Xi = 100$ (open stars), and $\Xi = 10^5$ (open triangles), exhibiting clearly the crossover from PB strictly repulsive pressure(solid line) at small values of Ξ to the SC prediction of attractions (broken line) at large Ξ. *A. G. Moreira, R. R. Netz (2001)*

2.1.2 Strong coupling theory

PB aproximation fails for $\Xi \gg 1$ (Figure 4). Let us observe different approach, called Strong coupling theory (SC) (its name is due to the fact that ions are strongly coupled between themselves, consequentially the coupling constant Ξ is large), which deals with the large counterion-counterion and counterion-macroion forces, being the consequence of high charge on the macroion and high valence of counterions. SC theory is given in a simplificated form valid only if isolated counterions are sandwiched between two charged plates of area A. Neglecting ion-ion interactions should be valid for $d \ll \sqrt{A}$. Denoting the distance between counterion and the plates as x and $d-x$, respectively, we obtain for the electrostatic interaction energies in units of k_BT the results $W_1 = 2\pi l_B z e_0 \sigma x$ and $W_2 = 2\pi l_B z e_0 \sigma(d-x)$. The sum of two interations is $W_{1+2} = W_1 + W_2 = 2\pi l_B z e_0 \sigma d$, which shows that i) no force is acting on the counterion since the forces exerted by two plates exactly cancels and ii) that the counterion mediates an effective attraction between the two plates. Because of $ze_0 = 2A\sigma$, the electrostatic repulsion between two plates is given by $W_{12} = -2\pi A l_B \sigma^2 d$, therefore the total electrostatic energy is $W_{el} = W_{12} + W_1 + W_2 = 2\pi A l_B \sigma^2 d$, leading to a negative electrostatic pressure

$$P_{el} = -\frac{\partial W_{el}/A}{\partial d} = -2\pi l_B \sigma^2. \tag{9}$$

The entropic pressure is a consequence of confinement of counterions between the plates. The gas law states $P = k_BT\rho$. Thus

$$P_{en} = \frac{1}{Ad}, \tag{10}$$

where pressure is in the units of $k_B T$. The total pressure is the sum of the attractive electrostatic and the repulsive entropic pressure.

$$P_{tot} = P_{el} + Pen = -2\pi l_B \sigma^2 + \frac{k_B T}{Ad} \tag{11}$$

According to SC theory, at small distances between plates entropic pressure prevails and the plates repel with the assimptotic behavior $P \sim 1/d$ at $d \to 0$, wheras at greater distances electrostatic potencial is greater and the plates attract themselves. The highest attraction possible is reached in the limit $d \to \infty$, where $P = -2\pi l_B \sigma^2$. SC prediction of a pressure as a function of distance between plates is shown on Figure 4 as a broken line.

2.1.3 Charged rods

Both approximations (PB and SC) can be applied to charged rods similarly as for charged plates above. Again, attraction between two charged rods surrounded with counterions occurs if rods are charged enough and if the valence of counterions is high enough. Monte Carlo simulations with charged rods instead of charged plates were made. Attraction interactions were observed. The results are given on the Figure 5. Attraction is observed in the cases for divalent and trivalent ions ($q_{rod} = -e/2$ and $q_{rod} = -e$, whereas only repulsion exists for univalent ions $q_{rod} = -e/4$. At higher rod separation the force diminish in all cases. This is because the SC theory is valid only for small separations. At large separations PB solution is adequate.

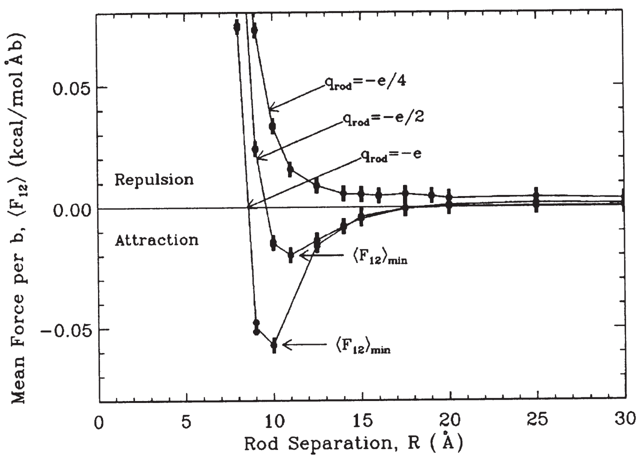

Figure 5: Mean force per lenght between two parallel charged rods, with divalent counterions, as a function of the rod separation distance R for different values of the rod charge. Obtained in the computer simulations. *N. G. Jensen, R. J. Mashl, R. F. Bruinsma, and W. M. Gelbart (1997)*

2.2 Free energy of the polyelectrolyte

Free energy of the polyelectrolyte may be written as a sum of elastic energy and electrostatic interaction energy. Elastic free energy can be expanded around the totally stretched molecule. It is linearly dependent on the square of the molecule's curvature ρ (definition for ρ is given in equation 22) [6]. Shape of molecule is parametrizated as $\mathbf{r}(s)$, where s is the length of the molecule. Total interaction energy can be described by monomer-monomer interaction potential $V(\mathbf{r}(s) - \mathbf{r}(s'))$, so that the total energy is given by

$$F = \frac{1}{2}K_c \int \left(\frac{\mathrm{d}^2\mathbf{r}}{\mathrm{d}s^2}\right)^2 \mathrm{d}s + \frac{1}{2}\iint \mathrm{d}s\mathrm{d}s' V(|\mathbf{r}(s) - \mathbf{r}(s')|) \qquad (12)$$

where K_C is elastic modulus, $K_c = k_B T L_P$. L_P is by definition persistence length of the molecule, which describes how stiff the molecule is (for DNA it is about 500 A). We have assumed, that potential $V(\mathbf{r}(s) - \mathbf{r}(s'))$ is not angle dependent.

Double helical structure makes DNA molecule relatively stiff. Sharp turns of molecule are not energetically favorable, in addition, confinement of the molecule in a very small volume decreases system's entropy. On the other hand, ionic interactions in special conditions attract and align different parts of DNA together. Toroid is the structure which fulfills these conditions in the highest degree, as we are about to show.

3 Structures of condensed DNA

3.1 Toroids

Experimentally, it is confirmed that DNA molecules under very different conditions condense in toroids. Condensation proceeds in presence of wide range of tri- and tetravalent cations, "bad solvent" (methanol, ethanol) and even some divalent cations. All toroids are characterized by the following structural features:

- the average radius of the toroid is about $500 \AA$ (the same as DNA persistence length);
- the cross section of the toroid is approximately circular, with a radius of $150 - 200 \AA$;
- the toroid is formed from circumferentially wound DNA, with local hexagonal packing of the parallel double strands.[2]

Still more remarkable than such structure being formed from a single molecule of DNA is the fact that similar toroids have been observed [7], when much shorter pieces of DNA are condensed by polyvalent cations. This molecules organize into "head-to-tail", circumferentially wound, hexagonally packed toroids having the same volume as the toroids formed from one large DNA (Figure 6).

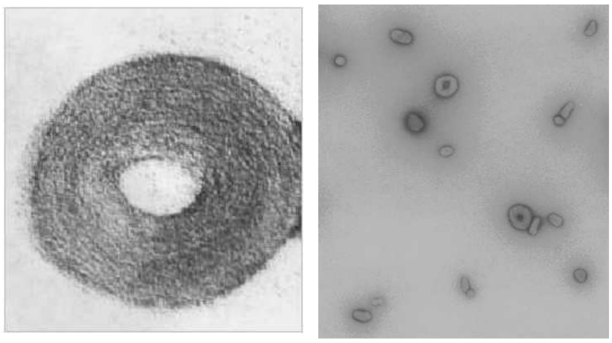

Figure 6: Toroidal structure of condensed DNA. Taken from *http:// www.csulb.edu/ gpickett/ Colloq01/ paco.jpg* and *http:// www.che.caltech.edu/ groups/ med/ images/ toroids.gif.*

3.2 Rods

A similar phenomenon of condensation is observed in the case of different much stiffer polyelectrolytes than DNA, such as F-actin (Figure 7), a principal structural protein in cells and in muscle tissue. Here the persistence length is almost two orders of magnitude larger than that of DNA. Consequently, the F-actins behave as essentially "rigid" rods. Upon the addition of polyvalent cations they condense into rodlike bundles. Under special conditions, especially in the presence of high concentration of alcohol, rods become predominant form also for DNA condensation as well, nevertheless under normal conditions rods are difficult to spot.

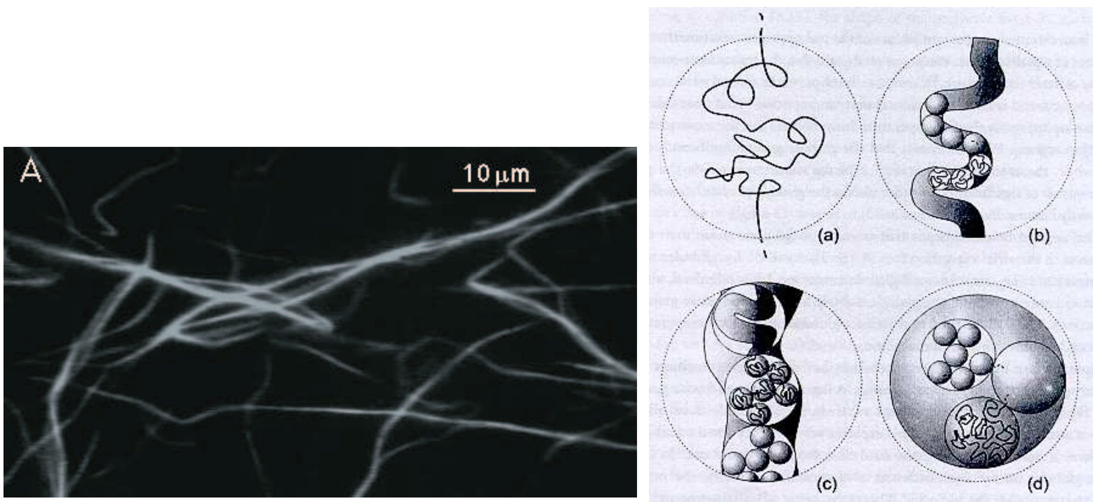

Figure 7: Other condensed structure caracteristic for (left) stiffer and (right) more flexible polyelectrolytes than DNA. Left: F-actin condensation to rodlike bundles. *http://expmed.bwh.harvard.edu /projects/polymer/actin_physics/actin_bundles.html* Right: Condensation of a flexible polimer. *A. Y. Grosberg, A. R. Khokhlov, (1997)*

In comparison, for a flexible polyelectrolyte with a small persistence length as opposed to the stiff polyelectrolyte such as DNA and even stiffer polyelectrolytes such as F-actin the coil-globule transition is not so abrupt. At the very start, lots of little "droplets" emerge, then they grow and merge with each other, until a larger spherical globule is formed (Figure 7).

3.3 Simple simulations of DNA condensation

Computer simulations of a simple, bead-spring model of semiflexible polyelectrolytes have been performed [1]. Different interaction potencials were included:

$$U = U_{LJ} + U_{bond} + U_C + U_{bend} \tag{13}$$

In the model the overlaping of ions is forbidden due to Lennard-Jones potencial, neighbouring ions on DNA molecule are connected with the elastic potencial, all charges interacted via Coulomb interactions. The sum over all counterions and ions on the coil is made. To achive apropriate stiffness of the coil, bending potential is introduced:

$$U_{bend} = k_1(\theta - \theta_0)^2 + k_2(\theta - \theta_0)^4, \tag{14}$$

being dependent on quadratic and quartic term of the angle difference between two naigboring ions on the coil.

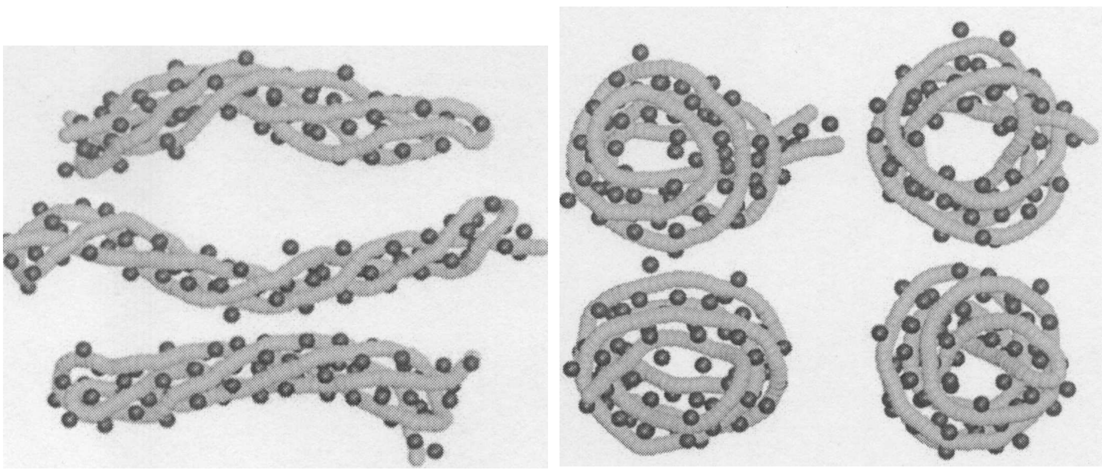

Figure 8: Images of condensed structures (toroids and rods) obtained from computer simulations. On the left rods are formed($k_1 = 20$,$k_2 = 0$), on the right picture rods are transformed to toroidal structure ($k_1 = 20$,$k_2 = 1500$). *M. J. Stevens (2001)*

The results are in agreement with experimental observations. Starting from extended, noncondensed conformations, condensed structures form in the simulations with tetravalent or trivalent counterions, while no condensate has been stable for divalent and monovalent counterions. Both toroidal and rod structures have occurred. The competition between them dependeds on whether a few sharper turns have required less energy than many slight bends. If the coil is relatively flexible ($k_1 = 20, k_2 = 0$), it is condensed to a rodlike bundles (left part of Figure 8), however, if the konstant k_2 is increased ($k_1 = 20, k_2 = 1500$), the rodlike bundles transform to the toroidal structures (right part of Figure 8).

4 Theory of toroid

4.1 Theory

Formally, the shape of DNA is determined by minimizing free energy written in equation (12). For chains under consideration, constrain of "inextensibility" has to be incorporated in the theory. Because the arc length of the curve equals to $\int_{s_1}^{s_2} \left(\frac{\partial \vec{r}}{\partial s}\right)^2 \mathrm{d}s = s_2 - s_1$, the constrain has the form

$$\left(\frac{\partial \vec{r}(s)}{\partial s}\right)^2 = 1. \tag{15}$$

Furthermore, interaction monomer-monomer potential is rewritten with the help of a field $B(s,s') = (\vec{r}(s) - \vec{r}(s'))^2$. The replacement

$$V(|\vec{r}(s) - \vec{r'}(s)|) \rightarrow V(B(s,s')) \tag{16}$$

is made.

By taking advantage of "Lagrange multiplier" technique , it is possible to minimize free energy from equation (12) in order to consider the constraint of "inextensibility"(Equations 15. Euler-Lagrange equations with respect to $\vec{r}$ lead to renormalisation of elastic constant K_C and the Lagrange multiplier λ in the following way:

$$\lambda \rightarrow \lambda + \delta\lambda, \tag{17}$$

$$K_C \rightarrow K_C + \delta K_C, \tag{18}$$

where the corrections δK_C and $\delta\lambda$ incorporporate interaction potencial $V(B(s,s'))$.

$$\delta\lambda = \int_0^L \mathrm{d}s s^2 V'(B(s)), \tag{19}$$

$$\delta K_C = -\frac{1}{12}\int_0^L \mathrm{d}s s^4 V'(B(s)). \tag{20}$$

After some manipulations one gets

$$\rho^2 = \frac{\delta\lambda}{K_C + \delta K_C}, \tag{21}$$

where $1/\rho$ is constant and represents the radius of the circle of curvature, which is defined as

$$\rho = |\ddot{\vec{r}}|. \tag{22}$$

4.2 Solenoid

Solenoid is the curve having the same radius of curvature along its trajectory. In this approximation the shape of DNA molecule is solenoid, which is given with the parametrization

$$\begin{aligned} x &= a \sin ws \\ y &= a \cos ws \\ z &= bws. \end{aligned} \tag{23}$$

Teh arc length of the solenoid is given by

$$\begin{aligned} s &= \int \sqrt{\dot{x}^2 + \dot{y}^2 + \dot{z}^2} w \mathrm{d}s \\ 1 &= w\sqrt{a^2 + b^2}, \end{aligned} \tag{24}$$

thus $w^2 = \frac{1}{a^2+b^2}$.

By calculating the circle of curvature of the solenoid ρ from the definition 22 and substituting it in the equation 21, the final equation is obtained. It connects parameter of solenoid with parameters of polyelectrolyte's interaction potencial V and its bedning modulus K_C.

$$\left(\frac{a}{a^2 + b^2}\right)^2 = \frac{\delta\lambda}{K_C + \delta K_C} \tag{25}$$

One has to solve this equation to get the form of the solenoid.

4.3 Numerical calculations

Parameter of solenoid b can be taken as the separation between DNA molecules. Having in mind a fact that DNA molecule is in condensed structure hexagonally packed b is of an order of DNA width $b = 4$nm. Parameter a can be numerically calculated from equation 25. It is assumed that to the lowest order

$$V(B) = -V_0 \exp(-\frac{\sqrt{B}}{L_\kappa}), \tag{26}$$

where L_κ is a characteristic length of the attractive interaction.

It can be seen from the Figure 10, that at small attractive potentials the coil is almost totally stretched. Only one solution for large values of the radius of the solenoid is obtained. If the size of the attractive potential given by V_0 is increased, the radious of the solenoid a is decreased. Suddenly, more solutions for a are possible. The free energy of both values for a should be calculated in order to predict the stable state. Two solutions for

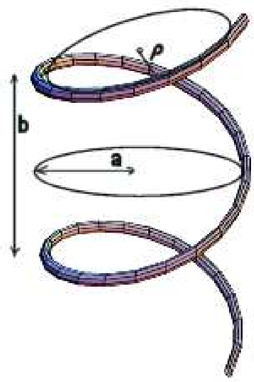

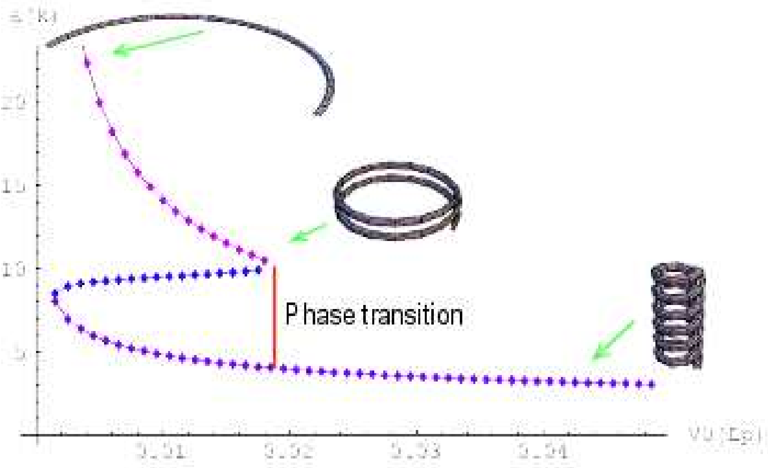

Figure 9: Parameters of the solenoid and the meaning of the radious of the curvature ρ.

Figure 10: Numerical calculations of DNA condensation from equation 25. The radius of solenoid a (in units of total length of the coil L) versus the strenght of attraction potential V_0 (in units of $k_B T$). Persistence length L_P of the molecule is the same as L_κ. The total length of the molecule is 50 times larger.

a exists until a reaches border value at about 0.2 of the total length of the coil L (Figure 10). After that, a first order phase transition happens and the radius a shrinks substantially. Thus the theory predicts the collapse of a DNA molecule as soon as the strength of the interaction potential V_0 is attractive enough, what can be experimentally achieved for instance by adding multivalent ions into the solution of DNA molecules, or by other mechanism.

5 DNA condensation *in vivo*

Most of the important biomolecules (for example, nucleic acids and proteins) are highly-charged objects in aqueous solution. Indeed, they need to be charged to avoid precipitation and phase separation at the high concentrations that characterize them in vivo. On the other hand, they still have to be packed in the small volume compared to their own size.

5.1 DNA in a bacteriophage

Viruses that infect bacteria are called bacteriophages - or "phages". Phage λ (Figure 11) consist of icosahedral protein capsid (2D cross-sections are hexagons) being attached to a hollow cylindrical "tail". Capsid contains

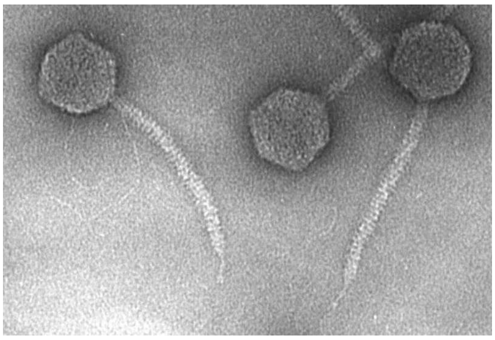

Figure 11: Left: Electron micrograph of Bacteriophage lambda λ. *http:// phage.bocklabs.wisc.edu/ Virus.htm*

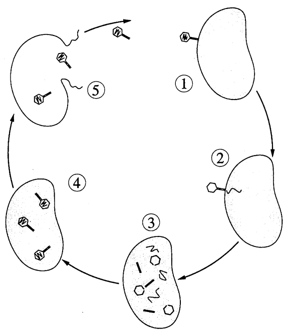

Figure 12: Right: Steps of the viral infection of a bacterial cell. *W. M. Gelbart (2001)*

only a single molecule of the viral DNA. Capsid radius is of the same order as DNA persistence length, therefore DNA has to be closely packed.

5.1.1 Viral infection

First, I review the process of viral infection of the bacteria (Figure 12). At the begining (1), the tail of the virus binds to its receptor protein in the bacterial membrane; in binding, the tail is opened and DNA is ejected (2) from the capsid into the cell interior. What drives this injection process is the high pressure of DNA in the capsid. Many copies of the DNA, viral capsids and tails are then made (3). Viral DNA is forced into each capsid by a special motor protein driven by ATP; the tail is joined onto the capsid (4). When a sufficient number (of the order of hundred) of viral particles have been replicated in this way, still another viral gene product serves to trigger lysis of the cell membrane (5). Each of the released viruses then attacks a new cell...

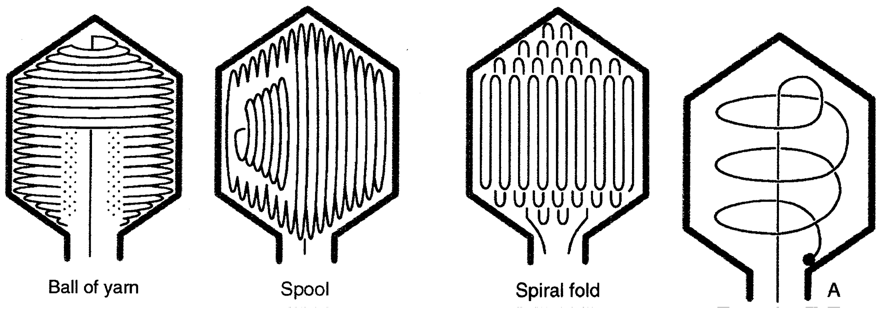

Figure 13: Three models for packaging of DNA in phage capsid on the left and a mechanism of DNA packing for the first model on the right. *V. A. Bloomfield, D. M. Crothers, I. Tinoco (2000)*

5.1.2 Structure of packaged DNA

The question that arises from rough description of infection process, is how the DNA is packed inside of a capsid in order to be able to eject itself rapidly without tangling. Experimental evidence has not provided a clear answer, but a few models have been proposed (Figure 13). Toroidal structure similar to that in caption 3.1 is present in two models. Possible mechanism for DNA packaging is shown on the Figure 13. Experimentally obtained energy required for packaging of DNA in the capsid can be compared to the calculated energy of our solenoidal approximation of the condensed shape. Comparison approximately confirms theoretical predictions of the packaging models.

6 Conclusion

It is very important biologically that the condensation mechanism is independent of the basepair sequence and more generally, the chemistry of DNA. Fitting DNA into small packages must be done independent of the genetic code it contains. Otherwise, some genetic sequences could not exist. The mechanism for formation of toroids described here depends solely on electrostatic interactions of charged ions on DNA and the counterions.

References

[1] M. J. Stevens: *Simple Simulations of DNA Condensation*, Biophysical Journal - Vol. 80, 130-139 (2001)

[2] W. M. Gelbart: *DNA Condensation and Complexation* published in *Electrostatic Effects in Soft Matter and Biophysics* edited by C. Holm, P. Kekicheff and R. Podgornik, Nato Science Series, II. Mathematics, Physics and Chemistry - Vol. 46, 53-85 (2001)

[3] A. G. Moreira, R. R. Netz: *Field-Theoretic Aproaches to Classical Charged Systems* published in *Electrostatic Effects in Soft Matter and Biophysics* edited by C. Holm, P. Kekicheff and R. Podgornik, Nato Science Series, II. Mathematics, Physics and Chemistry - Vol. 46, 317-364 (2001)

[4] P. L. Hansen, D. Svenšek, V. A. Parsegian, R. Podgornik: *Buckling, fluctuation and collapse in semiflexible polyelectrolytes*, Physical Review E, 60(2), 1956-1966 (1999)

[5] A. Y. Grosberg, A. R. Khokhlov: *Giant Molecules Here, There, and Everywhere*, Academic Press, (1997)

[6] L. D. Landau, E. M. Lifshitz: *Course of Theoretical Physics*, 3rd Edition, Butterworth-Heinmann (1999)

[7] V. A. Bloomfield, D. M. Crothers, I. Tinoco, JR.: *Nucleic Acids*, University Science Books (2000), 1471-1481 (1991)

[8] N. G. Jensen, R. J. Mashl, R. F. Bruinsma and W. M. Gelbart *Counterion-Induced Attraction between Rigid Polyelectrolytes*, Physical Review letters 74 (12), 2477-2480 (1997)

[9] B. Y. Ha, A. J. Liu (1999) *Kinetics of Bundle Growth in DNA Condensation* Europhysics Letters 46, 624-630